IRANIAN JOURNAL OF CATALYSIS

Montmorillonite-Zirconium Phosphate Catalysts for Methanol Dehydration

Hasanudin Hasanudin[a,b,*], Wan Ryan Asri[a,b], Qodria Utami Putri[a,b], Zainal Fanani[a,b], David Bahrin[c], Tuty Emilia Agustina[c], Karna Wijaya[d]

a) Department of Chemistry, Faculty of Mathematics and Natural Science, Universitas Sriwijaya, Inderalaya 30662, South Sumatra, Indonesia
b) Biofuel Research Group, Laboratory of Physical Chemistry, Faculty of Mathematics and Natural Science, Universitas Sriwijaya, Inderalaya 30662, South Sumatra, Indonesia
c) Department of Chemical Engineering, Faculty of Engineering, Universitas Sriwijaya, Inderalaya 30662, South Sumatra, Indonesia
d) Department of Chemistry, Faculty of Mathematics and Natural Science, Universitas Gadjah Mada, Yogyakarta 55281, Indonesia

Received 9 June 2022; received in revised form 25 July 2022; accepted 23 August 2022 (**DOI: 10.30495/IJC.2022.1960655.1942**)

ABSTRACT

Modification of sodium montmorillonite was conducted using zirconium phosphate. The effect of a series of phosphate precursors such as dihydrogen phosphate, diammonium hydrogen phosphate, and sodium phosphate was observed. The catalyst was used in the conversion of methanol dimethyl ether using 1 g of catalyst at a temperature range of 150-350 ˚C with a Liquid Hourly Space Velocity (LHSV) monitored to 2.54 h^{-1} and N_2 as carrier gas. The product was analyzed directly with a reactor system connected to gas chromatography. The X-ray diffraction (XRD), Scanning electron microscope-energy dispersive X-ray (SEM-EDX), N_2 adsorption-desorption, and Temperature-programmed desorption of ammonia (NH_3-TPD) were utilized to characterize the catalyst. The characterization showed that the modified sodium montmorillonite-zirconium phosphate was successfully synthesized. The study showed that modified montmorillonite using zirconium phosphate significantly increased the catalytic activity of sodium montmorillonite by providing medium and strong acid sites also increased the surface area. The modified sodium montmorillonite-zirconium phosphate from dihydrogen phosphate precursor exhibited the highest catalytic activity with the methanol conversion of 96.76%, dimethyl ether selectivity of 96.8%, and dimethyl ether yield of 93.67%, whereas the modified sodium montmorillonite-zirconium phosphate from diammonium hydrogen phosphate showed good stability towards methanol conversion.

***Keywords**: Methanol conversion, dimethyl ether, montmorillonite, zirconium phosphate*

1. Introduction

Fossil fuels are a major concern because they can cause environmental pollution and global warming. It is necessary to reduce the use of fossil fuels gradually and systematically in order to remedy these negative impacts [1–3]. One alternative fuel that could substitute fossil fuels is dimethyl ether (DME). DME produces less carbon, NO_x, and SO_x emissions than conventional fuels [4]. DME can be an environmentally friendly alternative fuel because its combustion produces fewer carbon emissions and exhaust gases containing NO_x and SO_x than conventional fuels [5]. Due to these advantages, the production of DME has attracted the attention of researchers [6].

Dimethyl ether can be produced by indirect and direct methods [7]. The indirect method is dimethyl ether production by gas synthesis with a hybrid catalyst [8], while the direct method is through methanol dehydration using an acid catalyst [9] such as sulfuric acid as a commercial catalyst [10]. However, it has disadvantages because it is corrosive and generates acid waste by-products. The disadvantages of a sulfuric acid catalyst in methanol dehydration have brought the attention of many researchers toward the development of alternative catalysts, especially heterogeneous

*Corresponding author:
E-mail address: hasanudin@mipa.unsri.ac.id (**H. Hasanudin**)

catalysts. Heterogeneous catalysts that have been studied include metal sulfates [11,12], metal nitride [13], and metal phosphate [14–18]. The use of metal phosphate as a catalyst for dehydration of methanol to DME has reasonably good performance, and it relies upon the sort of metal and the catalyst support used [17]. Some metals that are often used as catalysts for dehydration of methanol such as aluminum [14,15,17], boron [13], copper [11], cobalt [19] and zirconium [11,12,16,18]. These studies show that each metal has advantages as well as disadvantages depending on the form or precursor of the metal and what catalyst support is used.

Zirconium has high catalytic activity for the conversion of methanol to DME via dehydration. In this study, methanol dehydration was conducted with alumina-silica supported zirconium phosphate to improve the performance of zirconium phosphate catalysts. The use of alumina-silica as supporting material on methanol dehydration catalyst has been carried out using zeolite [20,21], ZSM-5 [22,23], alumina [24], kaolinite [25] and montmorillonite [26]. The results of these studies indicated that alumina-silica could improve the performance of the methanol dehydration catalyst. Montmorillonite can be used as catalyst support because it has a Lewis acid active site [27–29], which has a synergic effect with zirconium phosphate in the catalysis process of methanol dehydration.

According to Limlamthong et al. [17], different phosphate ions will give different acid strengths and properties. The character and strength of this acid will inherently determine the catalytic activity of the dehydration of methanol to DME [16]. To the best of knowledge, neither studies nor reports have yet been revealed regarding the effect of various sources of phosphate ions used (PO_4^{3-}, HPO_4^{2-} and $H_2PO_4^-$) on the methanol dehydration using montmorillonite-zirconium phosphate catalyst. In this study, the DME selectivity, DME yield, as well as methanol conversion would be investigated using a montmorillonite-zirconium phosphate catalyst with different phosphate precursors. The catalyst will be characterized using XRD, SEM-EDX, N_2 adsorption-desorption, and NH_3-TPD. The product was analyzed directly with a reactor system connected to gas chromatography.

2. Experimental

2.1 Materials

The materials used in this study were natural montmorillonite (Bayah area, Central Java, Indonesia), Sodium chloride (NaCl) (Merck, 99%), Silver nitrate ($AgNO_3$) (Merck, 99%), Zirconium (IV) oxide chloride octahydrate ($ZrOCl_2.8H_2O$) (Merck, 99%), Distilled water, Ammonium dihydrogen phosphate $(NH_4)H_2PO_4$ (Merck, 99%), Diammonium hydrogen phosphate $(NH_4)_2HPO_4$ (Merck, 99%), sodium phosphate (Merck, 99%), phosphoric acid (H_3PO_4) (Merck, 99%).

2.2 Preparation of catalyst

Na-montmorillonite (NaM) was prepared according to Wijaya et al. [30] using saturated NaCl. Substitution of Na^+ cations in the montmorillonite interlayer would increase the distance between the bentonite layers, and the cations would be more uniform [31]; consequently, modification of Na-montmorillonite will occur more nicely. Montmorillonite-zirconium phosphate was prepared using the wet impregnation method. 5 g of Na-montmorillonite was dispersed into 100 mL of 0.1 M $ZrOCl_2.8H_2O$ solution and added with distilled water until the volume became 250 mL. While stirring continuously, a phosphate solution (ammonium dihydrogen, diammonium hydrogen phosphate, and sodium phosphate) with a concentration of 1.25 M was added dropwise into this suspension and then stirred at ambient temperature for 1 day. After stirring, the temperature was incremented to 80 ˚C until the montmorillonite formed a paste. The paste was then calcined at 450 ˚C for 2 hours, washed with 0.5 M H_3PO_4 to remove Cl^- ions, and dried. The montmorillonite-zirconium phosphate from different phosphate precursors such as ammonium dihydrogen phosphate, diammonium hydrogen phosphate, and sodium phosphate was represented as M-ZrP1, M-ZrP2, M-ZrP3, respectively.

2.3 Characterization of catalyst

An APD 2000 Pro diffractometer (Cu Kα radiation with 15 kV, 10 mA) was used for X-ray diffraction analysis. The diffraction angle (2θ) was scanned from 5˚ to 80˚ intervals. The catalyst's textural properties were determined by performing an N_2 adsorption isotherm at 77 K using a NOVA 1000 Quantachrome. The morphology of the catalyst was observed with a scanning electron microscope (SEM) using JSM 6510 at an acceleration voltage of 20 kV. The distribution of total acidity and acid strength of the catalysts was determined by temperature-programmed desorption of ammonia (NH_3-TPD). The condition of NH_3-TPD analysis was prepared according to Palomo et al. [16], which was previously described.

2.4 Methanol dehydration

The continuous fixed bed reactor was used to investigate the catalytic activity of NaM, M-ZrP1, M-ZrP2, and M-ZrP3 catalysts on dimethyl ether production via dehydration of methanol. The volume capacity of the reactor was 196.40 L, with an inner diameter and length of 0.025 m and 0.4 m, respectively. The reaction was carried out using 1 g of catalyst at 150–350 ˚C temperature with a liquid hourly space velocity (LHSV) monitored to 2.54 h^{-1} using N_2 as a carrier gas. The product was analyzed directly with a reactor system connected to gas chromatography Perkin Elmer (model number 8700) equipped with an FID detector with a capillary column. The capillary temperature was kept above 150 °C using an electric heater to avoid the possibility of easily condensed molecules. The performance of the catalyst was evaluated by calculating the MeOH conversion, DME selectivity, and yield, according to equations (1–3) as follows:

$$\text{MeOH conversion} = \frac{X_o - X}{X_o} \times 100 \quad (1)$$

$$\text{DME Selectivity} = \frac{2 \times S_o}{X_o - X} \times 100 \quad (2)$$

$$\text{DME Yield} = \frac{2 \times S_o}{X_o} \times 100 \quad (3)$$

Where X_o was the initial of methanol moles, whereas X and S_o were the final of methanol and dimethyl ether moles produced, respectively.

3. Results and Discussion

3.1 Characterization of catalysts

The diffractograms of four catalysts such as NaM, M-ZrP1, M-ZrP2, and M-ZrP3 are shown in **Fig. 1**. The NaM diffractogram in **Fig. 1a** reveals typical peaks at 2θ of 6.15˚ and 19.69˚, which was corresponded to the montmorillonite mineral [32]. The reflection of basal spacing at 2θ of 6.15˚ was 13.08 Å which was supposed to the smectite clays typical (12 to 16 Å) [33]. The M-ZrP1, M-ZrP2, and M-ZrP3 diffractograms had sharp peaks in the 2θ of 15.53˚, 20.68˚, and 26.59˚, which indicated typical peaks of zirconium phosphates. These diffractions were relatively consistent with the monoclinic phosphate structure with a $P2_1/n$ space group [18]. Subsequently, there was a shift in the 2θ of zirconium phosphate relative to Na-montmorillonite; this occurred probably due to metal phosphate interaction with montmorillonite constituent. Furthermore, no significant changes were revealed in the 2θ peaks for the various phosphate precursors.

The surface morphology of the catalysts is shown in **Fig. 2**. The surface morphology of NaM in **Fig. 2a** appears to be thin wavy layers, which is typical of montmorillonite [34,35]. The surface morphology of NaM also showed a nearby layer and was regularly shaped with a slightly tight pore. Furthermore, the zirconium phosphate-montmorillonite's surface morphology had an irregular shape and looked roughly. Additionally, more small pores and foliated flakes were distributed on the surface due to montmorillonite modification by zirconium phosphate. According to Huang et al. [36], modification of layered materials such as clay would generate small pores on the clay's surface.

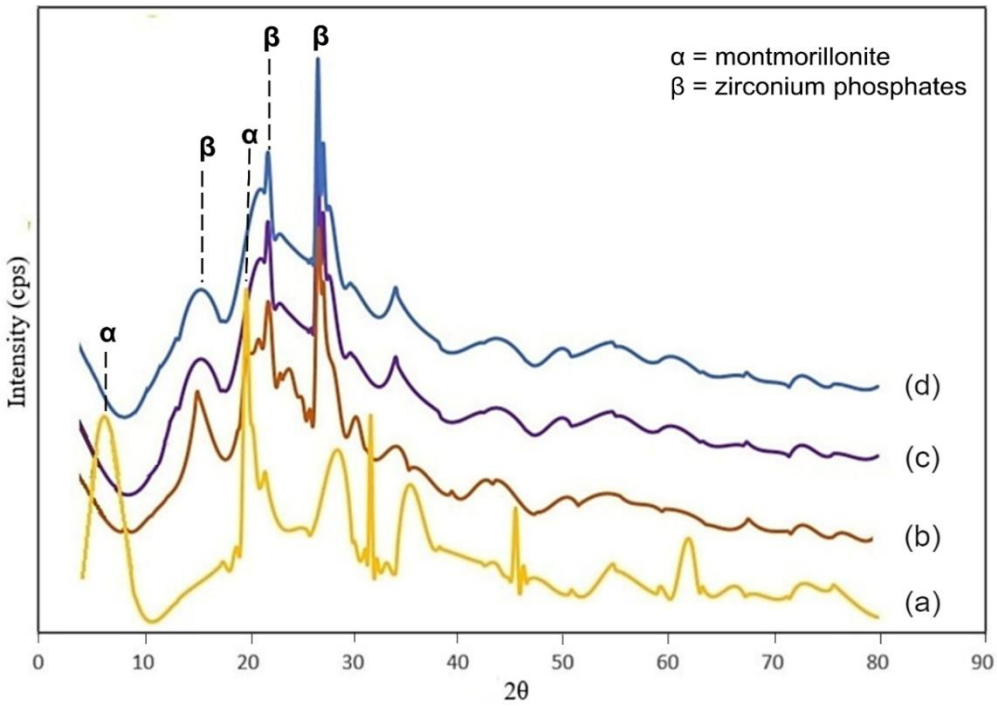

Fig. 1 XRD pattern of (a) NaM (b) M-ZrP1 (c) M-ZrP2 and (d) M-ZrP3 catalysts

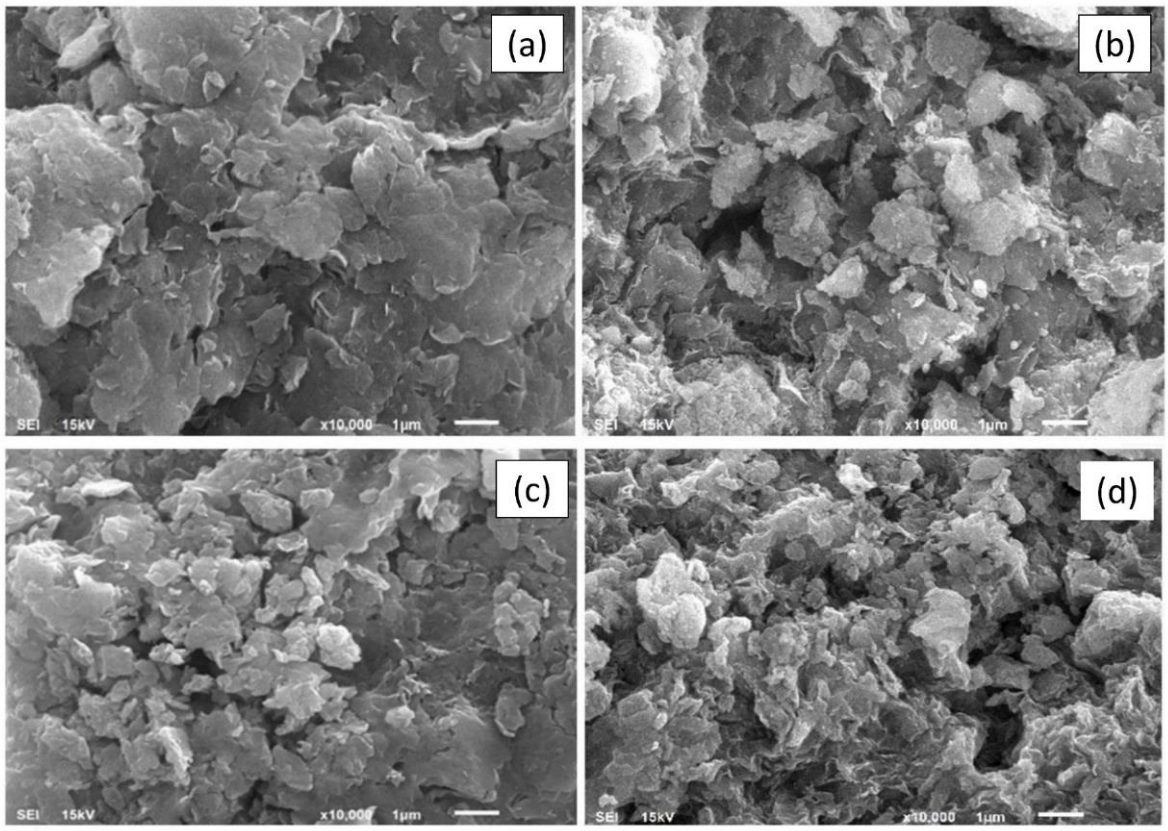

Fig. 2 SEM Images of (a) NaM (b) M-ZrP1 (c) M-ZrP2 and (d) M-ZrP3 catalysts

Subsequently, the EDX analysis of the catalyst is presented in **Table 1**. Obviously, there was an increase of phosphor as well as zirconium content after bentonite modification. Moreover, bentonite's Si/Al ratios decreased after modification using zirconium phosphate, which corroborated the success of bentonite's modification [37]. Furthermore, The sodium content of montmorillonite decreased after modification by zirconium phosphate, which is attributed to the maximum exchange of zirconium phosphate with sodium in montmorillonite [38]. Tomul [39] stated that the decrease of exchangeable cation, i.e., calcium, iron, and magnesium, suggested the successive bentonite's modification. The other impurities existed due to the natural circumstance of montmorillonite since it was taken from nature.

N_2 adsorption-desorption of catalysts is presented in **Fig. 3**. The adsorption of all catalysts demonstrated type II adsorption, which corresponded to the non-porous or macroporous catalyst with monolayer-multilayer adsorption [34]. The adsorption at low pressure was associated with monolayer circumstances. Thusly, a more continuous shape demonstrated covering of monolayer towards the commencement of multi-layer adsorption [40]. **Fig. 3** also shows that all catalysts had a type of H3 hysteresis loop, which indicated the presence of a non-rigid aggregate of plate-like particles, as well as a macropore that was not completely filled with pore condensate [41]. According to Ye et al. [42], the typical H3 hysteresis loop at P/P_o of 0.4 to 1 was demonstrated as the slit-shaped channels.

The textural properties of catalysts are presented in **Table 2**. It was clear that the modification using zirconium phosphate increases montmorillonite's surface area and pore volume. These conditions imply that zirconium phosphate had successfully modified montmorillonite through an intercalation mechanism [43,44]. This finding was consistently reported previously [38] with the study of bentonite modification using iron oxide. The M-ZrP1, M-ZrP2, and M-ZrP3 relatively did not have significantly different surface areas. The largest surface area was obtained by M-ZrP1 of 109.65 m^2/g. The previous report showed that molybdenum phosphide could increase the surface area of Na-bentonite from 52.84 to 63.69 m^2/g [28]. Marini et al. [45] reported that the H/bentonite and Ni/Al_2O_3/bentonite had a surface area of 79.08 and 37.63 m^2/g, respectively, whereas the Cr-ZrO_2-bentonite prepared by Wijaya et al. [47] had 105.80 m^2/g which is higher than as-prepared HF-bentonite (96.64 m^2/g). According to Bernard et al. [46], a high surface area promotes high catalytic activity.

Table 1. Element's content of catalysts.

Element	Content (wt%)			
	NaM	M-ZrP1	M-ZrP2	M-ZrP3
C	14.91	23.87	22.27	22.68
O	54.51	53.26	53.98	53.51
Al	6.28	3.11	4.21	4.46
Mg	0.68	0.32	0.44	0.45
Si	20.17	8.55	9.76	10.34
P	0	7.19	5.32	4.27
Cl	0	0.4	0.65	0.44
Ca	0.61	0.29	0.32	0.36
Fe	2.07	0.94	0.87	0.72
Na	0.78	0	0	0.65
Zr	0	2.07	2.18	2.12

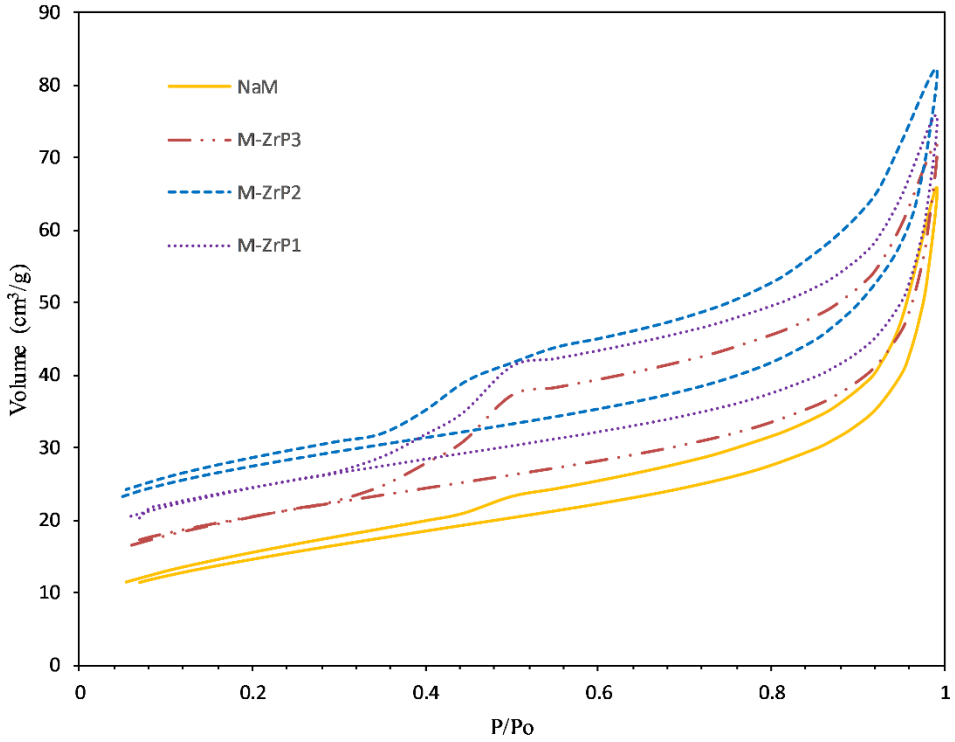

Fig. 3 N_2 adsorption desorption of catalysts

Table 2. Surface and pore properties of catalyst

Catalyst	Surface area (m^2/g)	Pore Volume (cm^3/g)	Pore Diameter (Å)
NaM	55.23	7.37×10^{-2}	53.38
M-ZrP1	109.65	1.56×10^{-1}	57.02
M-ZrP2	99.82	1.42×10^{-1}	61.79
M-ZrP3	95.64	1.35×10^{-1}	56.64

The ammonia-TPD results of the catalysts are shown in **Fig. 4**. It can be seen that the first peaks on all catalysts appeared at temperatures of 130–230 ˚C, which indicated the presence of weak acidic sites [48]. Those peaks probably corresponded to the ammonia molecule interaction between the Lewis acid site from the montmorillonite constituent through weak coordination bonds. Moreover, The peaks were seen to be higher after

the montmorillonite modification, which indicated the formation of new acidic sites from zirconium as well as phosphate group [16,49]. The second primary peak appears at 350–450 ˚C, which was revealed in the M-ZrP1 and M-ZrP2 catalysts. This peak appeared due to the desorption of ammonia that was bound to the Brønsted acid site with moderate strength [22]. The strong Brønsted acid sites on the M-ZrP1 and M-ZrP2 catalysts occurred due to the presence of dihydrogen phosphate and monohydrogen phosphate groups bound to the metal [50]. As can be seen in Fig. 4, the acidity properties of bentonite were remarkably enhanced, presumably due to the synergetic effect of the new Brønsted site acid presented by the P(OH) germinal groups as well as the Lewis acid promoted by the zirconium groups [51,52]. These acidic sites potentially increase the catalytic activity of catalyst towards dehydration reaction.

3.2. Catalytic Activity

The catalytic performance of the zirconium phosphate-montmorillonite catalyst with different phosphate precursors was evaluated for methanol dehydration to dimethyl ether (DME). Methanol dehydration was conducted with a vapor phase at 250 ˚C, 1 bar pressure, and LHSV of 2.56 hour^{-1} under steady conditions. **Table 3** shows the methanol conversion, DME selectivity and yield, respectively.

Table 3 revealed that the modification of montmorillonite using zirconium phosphate could enhance the catalytic activity of NaM significantly. Moreover, the catalytic performance of the catalyst was likely correlated to the phosphate precursors. The different phosphate precursors would generate different catalytic activity. **Table 3** clearly shows that the M-ZrP1 catalyst was much more active than the M-ZrP2 and M-ZrP3 catalysts in the methanol conversion. This condition was due to the acidic nature of the hydrogen ion on the catalyst, as well as the existence of medium and strong acid sites, which directly affect the activity of the catalyst in methanol dehydration [53]. This catalytic activity was consistent with the results of NH_3-TPD analysis as well as N_2 adsorption-desorption, which showed that the M-ZrP1 had the strongest acidic sides along with its highest surface area. Subsequently, the maximum yield of 96% DME was obtained by the M-ZrP1 catalyst, and this behavior could be described by the interaction of dihydrogen phosphate and zirconium as well as montmorillonite, which provided a synergistic effect, thereby providing additional active acid sites [54]. This result was not very significant compared to the M-ZrP2 catalyst but much higher than ZrP3 and NaM, due to the lack of acid active site that promotes the DME yield. It also revealed from **Table 3** that the high selectivity of zirconium phosphate-modified montmorillonite catalyst to DME (up to 93-96%) could be attributed to the presence of macropores in its structure due to modification by zirconium phosphate, which inherently increased the diffusion of the reactants and leads to the slight formation of by-products [23].

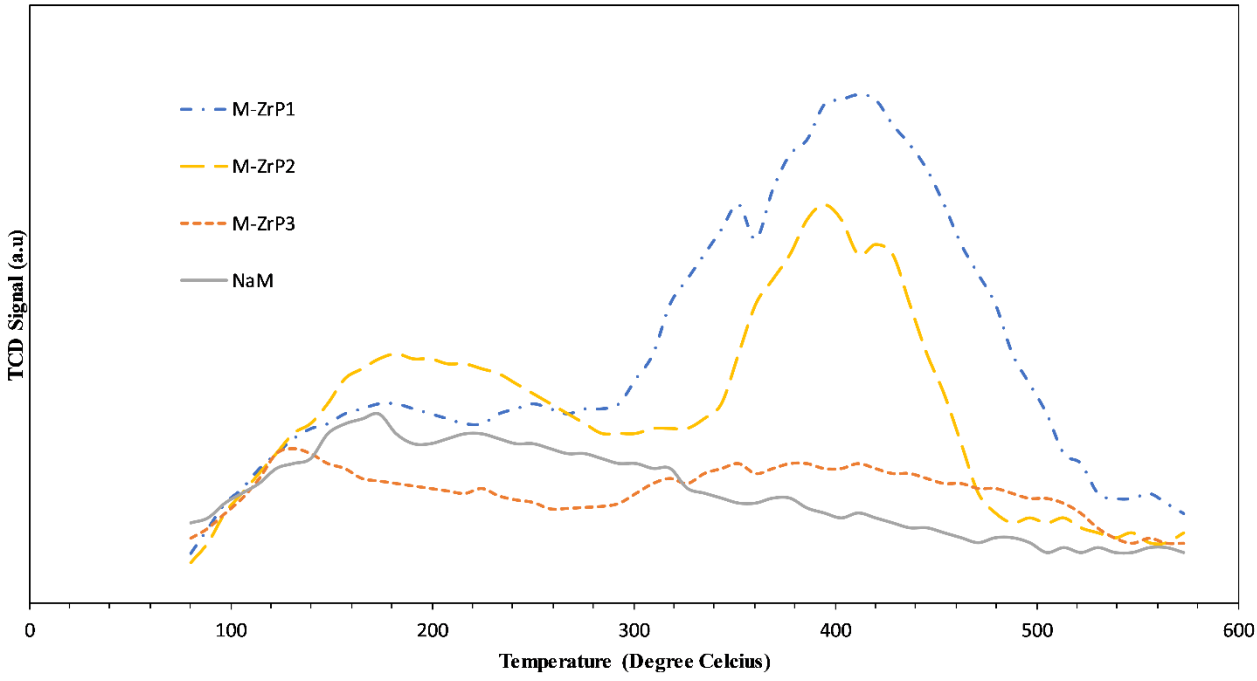

Fig. 4 NH_3-TPD of catalysts

Table 3. Methanol dehydration catalytic studies.

Catalyst	MeOH conversion (%)	DME selectivity (%)	DME yield (%)
NaM	12.69	52.31	6.64
M-ZrP1	96.76	96.8	93.67
M-ZrP2	92.32	96.65	89.23
M-ZrP3	65.52	93.33	61.15

The catalyst with the highest activity was then evaluated to check its stability and lifetime. The effect of time on stream to methanol conversion over M-ZrP1 and M-ZrP2 is shown in **Fig. 5**. The M-ZrP1 catalyst had better activity than M-ZrP2 but had lower stability than M-ZrP2. When the time on stream increases, the methanol conversion tends to decrease; the hydrocarbon formation such as coke could explain this phenomenon. The deactivation catalysts were primarily associated with either acid site coverage or clogged pores due to coke formation [55]. Coverage site closure, i.e., the deficiency of the active site by coked deposits, generating the active sites either pores or cavities, was inaccessible for catalyzing the methanol conversion. Reactants were adsorbed to the catalytic site within the pore, but when pores are clogged by deposits of carbon compounds on cavities or channel junctions, the pores cannot be accessed by the reactants [26]. It appears to be most of the strong acid sites in the M-ZrP1 catalyst are deactivated by pore-clogging, and the site of the medium and strong acids are responsible for catalyst stability. The medium/strong acid site of M-ZrP1 was more than M-ZrP2. Hence, the deactivation was more dominant in the M-ZrP1 catalyst.

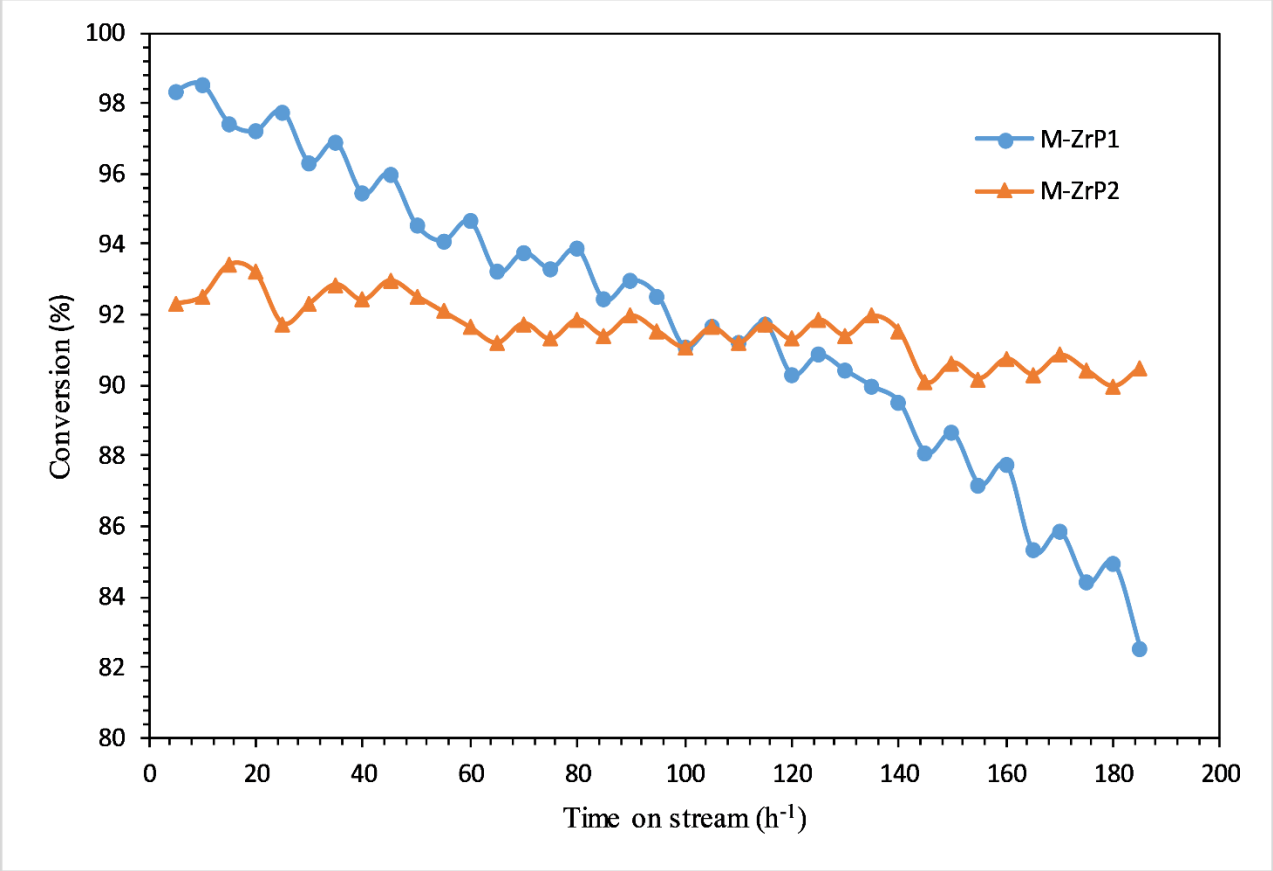

Fig. 5 Effect of time on stream to methanol conversion

4. Conclusions

The production of dimethyl ether (DME) via methanol dehydration was conducted over modified montmorillonite by zirconium phosphate catalysts. A series of zirconium phosphate-montmorillonite catalysts was evaluated including different phosphate precursors such as dihydrogen phosphate, diammonium hydrogen phosphate, and sodium phosphate which represent M-ZrP1, M-ZrP2, and M-ZrP3, respectively,. The study showed that the modification of Na-montmorillonite (NaM) using zirconium phosphate enhanced conversion methanol's catalytic activity, increased the NaM surface area, and provided a new strong acidic active site. The highest catalytic activity towards methanol conversion (96.76%), DME selectivity (96.8%), and DME yield (93.67%) was achieved by the M-ZrP1 catalyst, but it easily gets deactivated, whereas the M-ZrP2 catalysts showed good stability towards methanol conversion.

Acknowledgements

The author would like to express gratitude towards the Biofuel research group, Faculty of Mathematics and Natural Science, Universitas Sriwijaya, for the kind cooperation and encouragement that facilitated and completed this research.

References

[1] E.P. Sari, K. Wijaya, W. Trisunaryanti, A. Syoufian, H. Hasanudin, W.D. Saputri, Int. J. Energy Environ. Eng. 13 (2021) 967-978.
[2] S. Chu, A. Majumdar, Nature 488 (2012) 294–303.
[3] Z. Fanani, H. Hasanudin, A. Rachmat, M. Said, Molekul 16 (2021) 244–252.
[4] K.C. Tokay, T. Dogu, G. Dogu, Chem. Eng. J. 184 (2012) 278–285.
[5] Z. Azizi, M. Rezaeimanesh, T. Tohidian, M.R. Rahimpour, Chem. Eng. Process. Process Intensif. 82 (2014) 150–172.
[6] W.H. Chen, B.J. Lin, H.M. Lee, M.H. Huang, Appl. Energy 98 (2012) 92–101.
[7] F. Bahadori, M. Nalband Oshnuie, Sustain. Energy Technol. Assessments 31 (2019) 142–145.
[8] G.A. Olah, A. Goeppert, G.K.S. Prakash, J. Org. Chem. 74 (2009) 487–498.
[9] A.E.A.A. Said, M.A. El-Aal, J. Fuel Chem. Technol. 46 (2018) 67–74.
[10] S. Papari, M. Kazemeini, M. Fattahi, Chinese J. Chem. Eng. 21 (2013) 611–621.
[11] N.N. Petropavlov, G.M. Chalaya, I.G. Cygankova, A.L. Ilinskiy, E.L. Gagarinskiy, E.E. Fesenko, Biophysics 62 (2017) 158–163.
[12] A.E.A.A. Said, M.M. Abd El-Wahab, M.A. El-Aal, J. Mol. Catal. A Chem. 394 (2014) 40–47.
[13] J. Schnee, A. Eggermont, E.M. Gaigneaux, ACS Catal. 7 (2017) 4011–4017.
[14] F. Yaripour, F. Baghaei, I. Schmidt, J. Perregaarad, Catal. Commun. 6 (2005) 542–549.
[15] F. Yaripour, M. Mollavali, S.M. Jam, H. Atashi, Energy and Fuels 23 (2009) 1896–1900.
[16] J. Palomo, J. Rodríguez-Mirasol, T. Cordero, Materials 12 (2019) 2204.
[17] M. Limlamthong, N. Chitpong, B. Jongsomjit, Bull. Chem. React. Eng. Catal. 14 (2019) 1–8.
[18] I.O. Glukhova, E.A. Asabina, V.I. Pet'kov, E.Y. Mironova, N.A. Zhilyaeva, A.M. Kovalskii, A.B. Yaroslavtsev, Inorg. Mater. 56 (2020) 395–401.
[19] P.J. Skrdla, R.T. Robertson, J. Mol. Catal. A Chem. 194 (2003) 255–265.
[20] E. Catizzone, A. Aloise, M. Migliori, G. Giordano, Appl. Catal. A Gen. 502 (2015) 215–220.
[21] D. Masih, S. Rohani, J.N. Kondo, T. Tatsumi, Appl. Catal. B Environ. 217 (2017) 247–255.
[22] A.A. Rownaghi, F. Rezaei, M. Stante, J. Hedlund, Appl. Catal. B Environ. 119-120 (2012) 56–61.
[23] M. Rutkowska, D. Macina, N. Mirocha-Kubień, Z. Piwowarska, L. Chmielarz, Appl. Catal. B Environ. 174 (2015) 336–343.
[24] E. Catizzone, G. Bonura, M. Migliori, G. Braccio, F. Frusteri, G. Giordano, Tec. Ital. J. Eng. Sci. 63 (2019) 257–262.
[25] S. M. Solyman, M. A. Betiha, Egypt. J. Pet. 23 (2014) 247–254.
[26] M. Myrzakhanov, Y. Markayev, K. Shekeyeva, B. Utelbayev, J. Chem. Technol. Metall. 53 (2018) 31–36.
[27] H. Hasanudin, W. R. Asri, M. Said, P. T. Hidayati, W. Purwaningrum, N. Novia, K. Wijaya, RSC Adv. 12 (2022) 16431–16443.
[28] H. Hasanudin, W. R. Asri, K. Tampubolon, F. Riyanti, W. Purwaningrum, K. Wijaya, Pertanika J. Sci. Technol. 30 (2022) 1739–1754.
[29] H. Hasanudin, A. Rachmat, M. Said, K. Wijaya, Period. Polytech. Chem. Eng. 64 (2020) 238–247.
[30] K. Wijaya, E. Sugiharto, M. Mudasir, I. Tahir, I. Liawati, Indones. J. Chem. 4 (2010) 33–42.
[31] T. Hayakawa, M. Oya, M. Minase, K.I. Fujita, A.P. Teepakakorn, M. Ogawa, Appl. Clay Sci. 175 (2019) 124–129.
[32] M. Mirzan, K. Wijaya, I.I. Falah, W. Trisunaryanti, Asian J. Chem. 31 (2019) 229–234.

[33] J. Chanra, E. Budianto, B. Soegijono, IOP Conf. Ser. Mater. Sci. Eng. 509 (2019) 012057.
[34] M. Alshabanat, A. Al-Arrash, W. Mekhamer, J. Nanomater. 2013 (2013) 650725.
[35] A.R. Goodarzi, S.N. Fateh, H. Shekary, Appl. Clay Sci. 121-122 (2016) 17–28.
[36] Z. Huang, Y. Li, W. Chen, J. Shi, N. Zhang, X. Wang, Z. Li, L. Gao, Y. Zhang, Mater. Chem. Phys. 202 (2017) 266–276.
[37] M.S. Basiony, S.E. Gaber, H. Ibrahim, and E.A. Elshehy, Clays Clay Miner. 68 (2020) 197.
[38] A. Kadeche, A. Ramdani, M. Adjdir, A. Guendouzi, S. Taleb, M. Kaid, A. Deratani, Res. Chem. Intermed. 46 (2020) 4985–5008.
[39] F. Tomul, Appl. Surf. Sci. 258 (2011) 1836-1848.
[40] M. Thommes, K. Kaneko, A.V. Neimark, J.P. Olivier, F. Rodriguez-Reinoso, J. Rouquerol, K.S.W. Sing, Pure Appl. Chem. 87 (2015) 1051–1069.
[41] K.S.W. Sing, R.T. Williams, Adsorpt. Sci. Technol. 22 (2004) 773–782.
[42] R.P. Ye, W. Gong, Z. Sun, Q. Sheng, X. Shi, T. Wang, Y. Yao, J.J. Razink, L. Lin, Z. Zhou, H. Adidharma, J. Tang, M. Fan, Y.G. Yao, Energy 188 (2019) 116059.
[43] W. Huang, J. Chen, F. He, J. Tang, D. Li, Y. Zhu, Y. Zhang, Appl. Clay Sci. 104 (2015) 252–260.
[44] K. Wijaya, A.D. Ariyanti, I. Tahir, A. Syoufian, A. Rachmat, H. Hasanudin, Nano Hybrids Compos. 19 (2018) 46–54.
[45] A.T. Marini, K. Wijaya, and N.A. Sasongko, IOP Conf. Ser. Earth Environ. Sci. 124 (2018) 012009.
[46] K. Wijaya, A. Syoufian, A. Fitroturokhmah, W. Trisunaryanti, D. Adi Saputra, and Hasanudin, Nano Hybrids Compos. 27 (2019) 31-37.
[47] P. Bernard, P. Stelmachowski, P. Broś, W. Makowski, A. Kotarba, J. Chem. Educ. 98 (2021) 935–940.
[48] B. Mallesham, P. Sudarsanam, B.V.S.R. Reddy, B.G. Rao, B.M. Reddy, ACS Omega 3 (2018) 16839–16849.
[49] W. Wei, S. Wu, Fuel 225 (2018) 311–321.
[50] M.C. Alvarez-Galvan, J.M. Campos-Martin, J.L.G. Fierro, Catalysts 9 (2019) 293.
[51] R. Weingarten, Y.T. Kim, G.A. Tompsett, A. Fernández, K.S. Han, E.W. Hagaman, W.C. Conner, J.A. Dumesic, G.W. Huber, Catal. 304 (2013) 123-134.
[52] A. Sinhamahapatra, N. Sutradhar, B. Roy, A. Tarafdar, H.C. Bajaj, A.B. Panda, Appl. Catal. A Gen. 385 (2010) 22-30.
[53] G.R. Moradi, F. Yaripour, P. Vale-Sheyda, Fuel Process. Technol. 91 (2010) 461–468.
[54] W. Ni, D. Li, X. Zhao, W. Ma, K. Kong, Q. Gu, M. Chen, Z. Hou, Catal. Today 319 (2019) 66–75.
[55] K. Yoo, P.G. Smirniotis, Appl. Catal. A Gen. 246 (2003) 243–251.